Vol. 149: 59–70, 2022
https://doi.org/10.3354/dao03662

DISEASES OF AQUATIC ORGANISMS
Dis Aquat Org

Published online May 24

Diffuse large B cell lymphoma and a novel gammaherpesvirus in northern elephant seals *Mirounga angustirostris*

Margaret E. Martinez[1,*], Nicole I. Stacy[2], James F. X. Wellehan Jr.[2], Linda L. Archer[2], Salvatore Frasca Jr.[3], Carlos Rios[1], Emily J. Trumbull[1,4], Michelle Rivard[1], Emily R. Whitmer[1], Cara L. Field[1], Pádraig J. Duignan[1]

[1]The Marine Mammal Center, Sausalito, California 94965, USA
[2]College of Veterinary Medicine, University of Florida, Gainesville, Florida 32608, USA
[3]Connecticut Veterinary Medical Diagnostic Laboratory, Department of Pathobiology and Veterinary Science, University of Connecticut, Storrs, Connecticut 06269, USA
[4]SeaWorld, San Antonio, Texas 78251, USA

ABSTRACT: Two emaciated male northern elephant seal (NES) *Mirounga angustirostris* pups were admitted to The Marine Mammal Center (Sausalito, California, USA) and treated for malnutrition. Complete blood counts showed a progressive moderate to marked leukocytosis characterized by a predominance of large monomorphic mononuclear cells of probable lymphoid origin, frequently with flower-shaped nuclei. Both seals were euthanized due to suspected lymphoid neoplasia. At necropsy, most lymph nodes in both pups were markedly enlarged, some with distinct white nodules, the spleens were diffusely enlarged, and the intestinal mucosae were thickened. Histopathologic features consistent with disseminated large cell lymphoma were identified to varying degrees of severity in lymph nodes, bone marrow, liver, tonsils, spleen, liver, intestines, kidneys, lower urinary tract, and several other organs. Immunohistochemical staining of neoplastic cells was most consistent with B lymphocyte origin, with most cells staining positively for Pax 5 and CD20 with admixed small CD3-positive T lymphocytes and CD204-positive macrophages. PCR and sequencing identified a novel gammaherpesvirus, herein called miroungine gammaherpesvirus 3, from affected tissues. This virus is in a clade outside of named genera that utilize hosts in the suborder *Caniformia*. The present study is the first description of diffuse large B cell lymphoma with leukemic manifestation and concomitant detection of a novel gammaherpesvirus in free-living NESs. Further research regarding the prevalence of this new gammaherpesvirus and its associated pathogenesis in this species is indicated.

KEY WORDS: Northern elephant seal · *Mirounga angustirostris* · Lymphoma · *Gammaherpesvirinae* · Leukemia · B cell · Immunohistochemistry

1. INTRODUCTION

Northern elephant seals (NESs) *Mirounga angustirostris* are phocid seals native to the eastern and central North Pacific, with major breeding colonies on the California, USA, coast. The breeding season extends from December through March, and pups are weaned abruptly around 4 wk post-partum after which they remain at the natal site for several more weeks before dispersing from the colony. While on land, they are in close contact with cohorts and NESs of different age classes. The species went through a

*Corresponding author: martinezm_fellow@tmmc.org

Publisher: Inter-Research · www.int-res.com

severe genetic bottleneck in the 19th century due to hunting that reduced the population to as few as 20–100 individuals (Weber et al. 2000). However, since federal protection was initiated in 1972, the population has increased to over 200 000 (Lowry et al. 2014, Spraker et al. 2019). Limited studies on the health of free-living NESs have documented the most frequent causes of mortality in pups and juveniles as trauma, bacteremia/septicemia, emaciation, and congenital abnormalities (Trupkiewicz et al. 1997, Spraker et al. 2014). Other documented causes of death in stranded animals under rehabilitation include malnutrition, *Otostrongylus circumlitus*-associated pulmonary hemorrhage, congenital defects, and NES skin disease (Colegrove et al. 2005). However, neoplasia is rarely diagnosed, with only one known report of biliary carcinoma in an adult female (Beckmen et al. 1997, Fauquier et al. 2003).

Herpesviruses are a family of viruses with high host fidelity and a low evolutionary rate; jumping between hosts is uncommon as they usually appear to coevolve with their host species (Davison 2011). Two herpesviruses have been previously identified in NESs under rehabilitation, both in the subfamily *Gammaherpesvirinae*. The first, called northern elephant seal herpesvirus (and herein referred to as northern elephant seal gammaherpesvirus 1 [NES GHV1]), was identified in a juvenile NES with oral ulceration (Goldstein et al. 2006). The second, phocid herpesvirus 6 (PhHV6), was identified from ocular swabs in 3 of 18 NESs (Wright et al. 2015) and not associated with any specific pathology. Incidentally, this virus was also found in one of 34 harbor seals (HSs) *Phoca vitulina* at the same rehabilitation facility (Wright et al. 2015).

Several viruses have been identified in association with lymphoma or leukemia such as feline leukemia virus and feline lymphoma and Epstein Barr virus in humans (Nicholas 2000, Rajčáni et al. 2010, Rosenwirth et al. 2011, Beatty 2014, Panfil et al. 2016, Casulo & Friedberg 2018). Oncogenic gammaherpesvirus infections have been documented in pinnipeds, with the clearest association between otariid gammaherpesvirus 1 (OtGHV1), containing viral oncogenes, and urogenital carcinoma in California sea lions (CSLs) *Zalophus californianus* (Buckles et al. 2006, Gulland et al. 2020, Deming et al. 2021). Another gammaherpesvirus, otariid gammaherpesvirus 3 (OtGHV3), was found in lymphocytes in a CSL with multicentric large B cell lymphoma (Venn-Watson et al. 2012). Suspect enveloped viral structures were also present in a northern fur seal (NFS) *Callorhinus ursinus* pup with multicentric large cell lymphoma (Stedham et al. 1977). This report describes the occurrence of B cell lymphoid neoplasia in association with a novel gammaherpesvirus in 2 NES pups during rehabilitation at The Marine Mammal Center (TMMC) that stranded a year apart.

2. MATERIALS AND METHODS

2.1. Physical examination and blood analysis

Both lymphoma cases were male NES pups rescued due to emaciation along the central California coast: Case 1 stranded at Estero Bluffs in Cayucos (35.4493° N, 120.9186° W) in 2020; Case 2 stranded at Manresa State Beach (36.9322° N, 121.8630° W) in 2021. Control cases 1–3 stranded along the response range of TMMC including Santa Cruz County (Control 1 and 2), and Esteros Bluffs in Cayucos (Control 3) in 2021 (Control 1) and 2019 (Controls 2 and 3). Control cases were selected based on time of stranding related to the lymphoma cases as well as those with a complete necropsy, histopathology, and similar sampled tissues for viral genomic testing. Routine physical examination on all animals included evaluation of cardiovascular, respiratory, musculoskeletal, nervous, urogenital, gastrointestinal, and ocular systems. Hematology and serum biochemistry analyses were performed using a SCIL Vet ABC Plus hematology analyzer (SCIL Vet America). Blood smears from both cases and postmortem lymph node impression smears from Case 1 were stained using Wright Giemsa stain (Harleco®, EMD Millipore). Hematologic reference ranges were previously established at TMMC (Gulland et al. 2018).

2.2. Gross pathology and histopathology

Complete necropsies were performed within 72 h of euthanasia, and tissues were fixed with 10% neutral buffered formalin, trimmed, and routinely processed for paraffin embedding. Histologic sections were prepared at 5 µm and stained with hematoxylin and eosin (H&E) at the University of California, Davis, College of Veterinary Medicine (UC Davis CVM).

2.3. Immunocytochemistry (ICC) and -histochemistry (IHC)

ICC was performed by fixing blood films and impression smears in acetone at the University of

Florida College of Veterinary Medicine using a Bond RX fully automated research stainer (Leica Biosystems). Cytology slides were stained using a monoclonal mouse anti-IBA-1 antibody (cat #MABN92, Millipore) (1:300), a monoclonal mouse anti-CD3 (cat #NCL-L-CD3-565 clone LN10, Leica) (1:75), and a polyclonal rabbit anti-CD79a (cat # PA5-32333, ThermoFisher) (1:75) with a Leica bond polymer refine red detection kit (cat # DS9390, Leica). Staining demonstrated few small lymphocytes with diffuse strong cytoplasmic CD3 labeling and no IBA-1 labeling of neoplastic cells. CD79a labeling could not be interpreted as there was labeling in the secondary-only control.

IHC was performed at UC Davis CVM on paraffin-embedded formalin-fixed tissues using an in-house monoclonal IgG1 rat anti-CD3 (10:100), a monoclonal mouse anti-CD204/SRA-E5 (cat #KT022, Transgenic) (1:200), a polyclonal rabbit anti-CD20 NeoMarker (cat #RB-9013-P1, NeoMarker) (1:300), a monoclonal mouse anti-CD79a/HM57 (cat#MCA2538H, AbDSero) (1:100), and a monoclonal mouse anti-PAX5 (cat #BD610863, BD Biosciences) (1:100). The anti-CD3, CD20, CD79a, and PAX5 received HIER in a citrate buffer, the anti-CD204 received HIER EDTA buffer at a pH of 9. The secondary antibodies used included goat anti-rat (Cat #30033, Vector Labs) for the CD3 protocol, and Mouse-on-Canine HRP-Polymer (cat #MC541, Biocare) for the CD204, CD79a, and PAX5 protocols, and Rabbit-on-Canine HRP-Polymer (cat #RC542, Biocare) for the CD20 protocol. Secondary antibody-only controls were used, as well as a control canine lymph node on each slide stained with the various antibodies to verify correct labeling/staining and to evaluate non-specific staining. To fully evaluate non-specific staining, isotype control antibodies were also used. To confirm appropriate labeling of the affected tissues and to evaluate the effect neoplasia had on normal lymph node architecture, normal lymph node and spleen from an unaffected NES pup were labeled with the antibodies.

2.4. Transmission electron microscopy (TEM)

The formalin fixed pulmonary lymph node from Case 1 was postfixed in 3% glutaraldehyde (Electron Microscopy Microscopy Sciences), embedded, sectioned, and stained by routine methods for TEM as previously described (Cianciolo et al. 2013).

2.5. PCR and sequencing

To determine if there was a viral association with the B cell lymphoid neoplasm, DNA was extracted using a DNeasy Kit (Qiagen) from spleen and lymph node from both cases, as well as spleen and/or lymph nodes from 3 unaffected NES pups that had been frozen and stored in RNAlater (Cat# AM7021, Invitrogen). Nested PCR amplification of a partial sequence of the herpesviral DNA-directed DNA polymerase gene (pol) was performed using methods described in (VanDevanter et al. 1996). The product was resolved on a 1% agarose gel and purified using the QIAquick Gel Extraction Kit (Qiagen). Direct Sanger sequencing was performed using the Big-Dye Terminator Kit (Applied Biosystems). To obtain additional sequence for phylogenetic comparison, further amplification used primers DIEC, SIIQ, and IYG (Maness et al. 2011), and products were sequenced as above. Primer sequences were edited prior to sequence alignment and phylogenetic analyses.

2.6. Phylogenetic analysis

Predicted homologous 229–282 amino acid (AA) sequences of 70 herpesvirus DNA-dependent-DNA polymerase were aligned using MAFFT (Katoh & Toh 2008). Partial homologous AA sequences for which full-length was not available were included, with ambiguities added for unknown AAs. Chelonid alphaherpesvirus 5 (GenBank acc. no. YP_009207091) was selected as the outgroup. Bayesian analyses of each alignment were conducted using Mr. Bayes 3.2.6 on the CIPRES server with mixed AA substitution models, gamma distributed rate variation, and a proportion of invariable sites (Ronquist et al. 2012, Miller et al. 2015). A total of 4 chains were run, and statistical convergence was assessed via the average standard deviation of split frequencies and potential scale reduction factors of parameters. The initial 25% of 2 000 000 iterations were discarded as burn in.

3. RESULTS

3.1. Clinical presentation

The first male NES pup (Case 1) stranded in April of 2020 near San Luis Obispo, California. The second male NES pup (Case 2) stranded in April of 2021 near Santa Cruz, California. Both were emaciated, based on the absence of sub-cutaneous adipose tissue.

Case 1 also presented with ventral fold dermatitis (Fig. S1a in the Supplement at www.int-res.com/articles/suppl/d149p059_supp.pdf) that progressed despite antibiotic treatment (ceftiofur crystalline [Excede® 200 mg ml^{-1}, Zoetis] 6.6 mg kg^{-1} SC one time; ciprofloxacin [Parke-Davis, Pfizer]; 14.2 mg kg^{-1} PO once daily for 3 wk, and cephalexin (Aurobindo; 750 mg PO BID for 1 wk). Skin impression smears revealed numerous, mostly rod-shaped, bacteria, granulocytes, and small to large lymphocytes.

Hematology and serum chemistry on Case 1 showed a mild-moderate lymphocytic leukocytosis (39.8 × 10^3 mm^{-3}), markedly elevated gamma-glutamyl transferase (GGT), and mildly elevated alkaline phosphatase 3 d post-rescue (Table S1). This animal showed improved mentation, activity, and appetite during the first 2 wk in care, then declined in the last week. In conjunction with the clinical decline, leukocytosis progressed from mild-moderate to marked (131.7 × 10^3 mm^{-3}) by the day of euthanasia (20 d post-rescue). In addition, there was a sudden onset of marked thrombocytopenia (56 × 10^9 l^{-1}), moderately increased blood urea nitrogen (BUN), and mild to marked elevations in other biomarkers as evidence of acute hepatocellular injury on the day of euthanasia (Table S1). At euthanasia, the superficial cervical lymph nodes were palpably enlarged (approximately 8 cm diameter).

Case 2 presented with multiple small puncture wounds and lacerations due to a reported dog interaction. Significant hematologic abnormalities on admission clinical examination (3 d post-rescue) included a moderate lymphocytic leukocytosis (52.6 × 10^3 mm^{-3}), a markedly low platelet count (39 × 10^9 l^{-1}), markedly elevated GGT and bilirubin (6.3 mg dl^{-1}) (Table S1). Peripheral lymph nodes were not palpable at the initial clinical examination. This pup was more debilitated than Case 1 and declined rapidly over the 5 d in care; therefore, euthanasia was elected.

Blood smears from both cases revealed frequent intermediate to large lymphocytes occasionally with 'flower-like' nuclear morphology, with the majority of nuclei 2.5–4 times the diameter of red blood cells. The centrally located nuclei were round, oval, binucleated, or multilobed with smooth purple chromatin and one to multiple, variably distinct, round to oval or elongated nucleoli (Fig. 1a). Occasional mitotic figures were noted. Cytoplasm was scant to moderate in volume, variably basophilic and occasionally vacuolated or contained a pale perinuclear clear zone. Also present were low numbers of small well-differentiated lymphocytes, segmented and band neutrophils, monocytes, and nucleated red blood cells. This morphology was present on blood smears 15 d post-rescue for Case 1 and 3 d post-rescue for Case 2. Euthanasia was elected based on the clinical decline of the pups as well as the clinicopathologic findings indicative of lymphoid neoplasia.

Control 1 presented with increased respiratory effort and a moderate leukopenia (6.1 ×10^3 mm^{-3}) and a left shift. The primary clinical differential was aspiration pneumonia, confirmed on necropsy, and 8 d after presentation the pup was euthanized due to a poor response to treatment. Control 2 presented lethargic with a moderate leukocytosis (44.7 × 10^3 mm^{-3}), neutrophilia (97% segmented neutrophils), moderate thrombocytopenia (96 ×10^9 l^{-1}), marked bilirubinemia (10.7 mg dl^{-1}), and mild to moderate elevations in hepatocellular and biliary system markers consistent with otostrongyliasis. Due to the poor prognosis, Control 2 was euthanized 2 d after presentation, and otostrongyliasis was confirmed on necropsy. Control 3 presented with kyphosis which radiography demonstrated to be due to traumatic injury and displacement of multiple vertebrae and was confirmed by necropsy. While Control 3 had few hematologic or blood chemistry abnormalities, the patient failed to respond to treatment and was humanely euthanized after 12 d in care.

3.2. Necropsy findings

At necropsy, the lymph nodes of Case 1 were markedly enlarged, firm, bulging and homogenous on cut surface (Fig. 1b). Similarly, the tonsils, spleen, and thymus were diffusely firm and enlarged. The jejunum, ileum, and most notably the colon, had dark red, thickened, corrugated mucosa with distinct white firm nodules. There were also multiple linear ulcerations of the ventral abdominal skin folds with granulation tissue and minimal fibrinosuppurative exudate (Fig. S1a), as well as a thickened, multinodular, and congested urinary bladder mucosa. Case 2 had similar necropsy findings except that the urinary bladder mucosa and thymus were not affected. In addition, many lymph nodes of Case 2 had distinct intraparenchymal homogenous white firm bulging nodules (Fig. 1c). The small and large intestines of Case 2 were similarly thickened and corrugated but were diffusely tan rather than dark red as in Case 1 (Fig. 1d). In Case 2 there was a single well-demarcated oral ulceration (7 mm diameter) on the hard palate (Fig. S1c) and moderate icterus. *Otostrongylus circumlitus*-associated vasculitis was not present in either case.

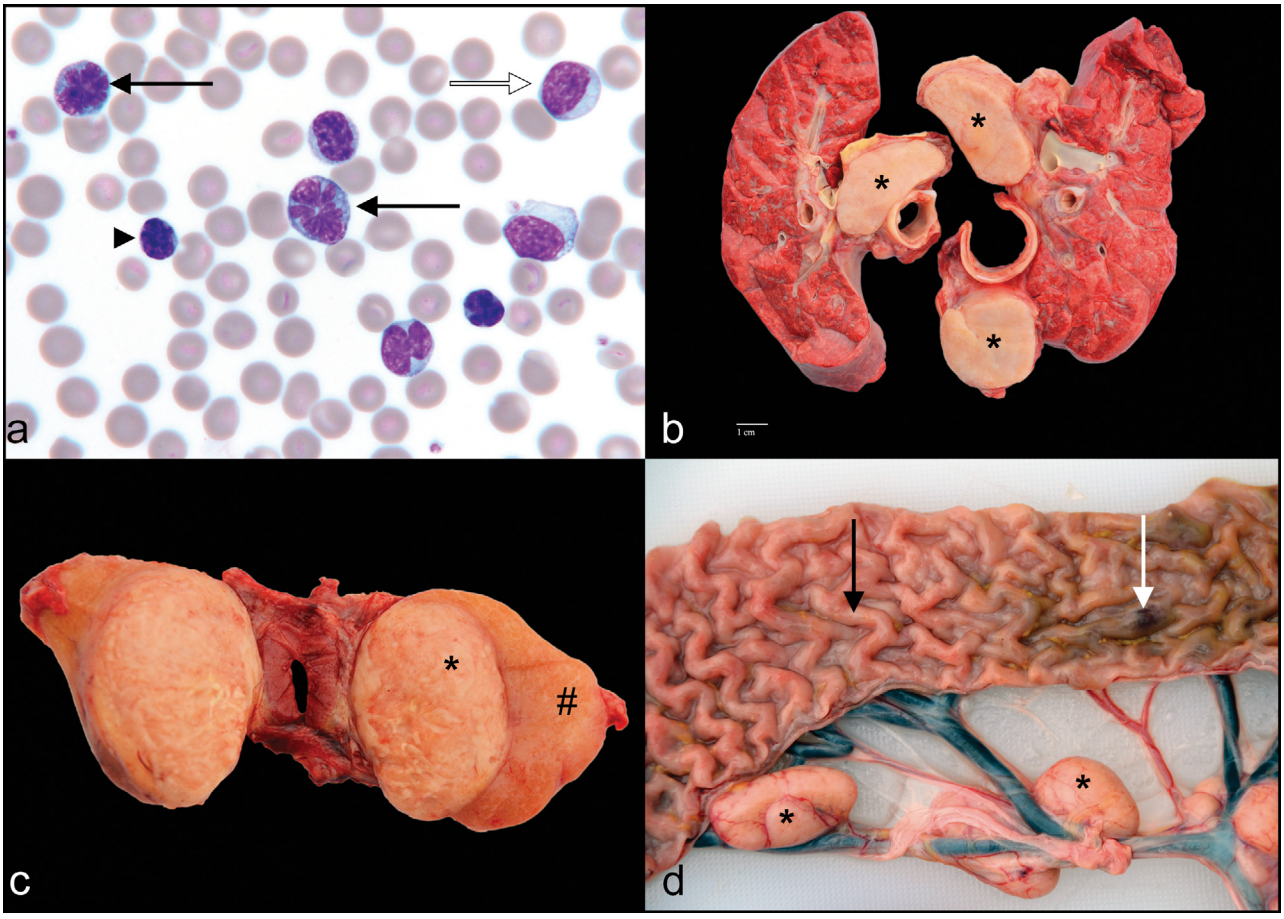

Fig. 1. (a) Case 1. Blood smear, Wright Giemsa. Neoplastic lymphocytes with flower-like nuclei (black arrows), large mononuclear lymphocytes (white arrow) and fewer small to intermediate sized lymphocytes (arrowhead). (b) Case 1. Tracheobronchial and pulmonary lymph nodes. Lymph nodes (asterisks) are enlarged and effaced by neoplastic tissue. (c) Case 2. Cross section of the enlarged left submandibular lymph node. A well-demarcated oval pale tan neoplastic nodule (asterisk) is distinct from the adjacent normal lymph node parenchyma (hashtag). (d) Case 2. Colon and colonic lymph nodes. The colonic mucosa is corrugated with thickened pale tan mucosa (black arrow) and random foci of mucosal hemorrhage (white arrow). Colonic lymph nodes are enlarged (asterisks)

3.3. Postmortem cytology

Impression smears of the mesenteric lymph node from Case 1 obtained at postmortem examination were stained with Wright Geimsa stain. The tissue imprints were highly cellular with numerous large neoplastic lymphocytes similar to those described above for blood smears (Fig. 2a). Occasional mitotic figures or binucleation were present with lesser numbers of small, well-differentiated lymphocytes and few histiocytes.

3.4. Histopathology

On histopathologic examination of Case 1, all lymph nodes and the tonsils had approximately 90% of the normal follicular architecture effaced by diffusely infiltrative sheets of neoplastic round cells that often invaded through the capsule (Fig. 2b). Well-differentiated small to intermediate lymphocytes were compressed to the periphery by sheets of neoplastic cells. The small well-differentiated lymphocytes were also admixed with the neoplastic round cells, comprising approximately 20–40% of the cellular population. Neoplastic cells were round, had moderately distinct cell borders, scant to moderate amphophilic cytoplasm, and a single round to reniform nucleus with 1 or 2 prominent nucleoli and dispersed chromatin (Fig. 2c). Neoplastic cell nuclei were 2× the diameter of an erythrocyte (interpreted as large cell). There was marked anisocytosis and anisokaryosis with rare binucleation. There was an average of 13 mitotic figures in a field of view area of

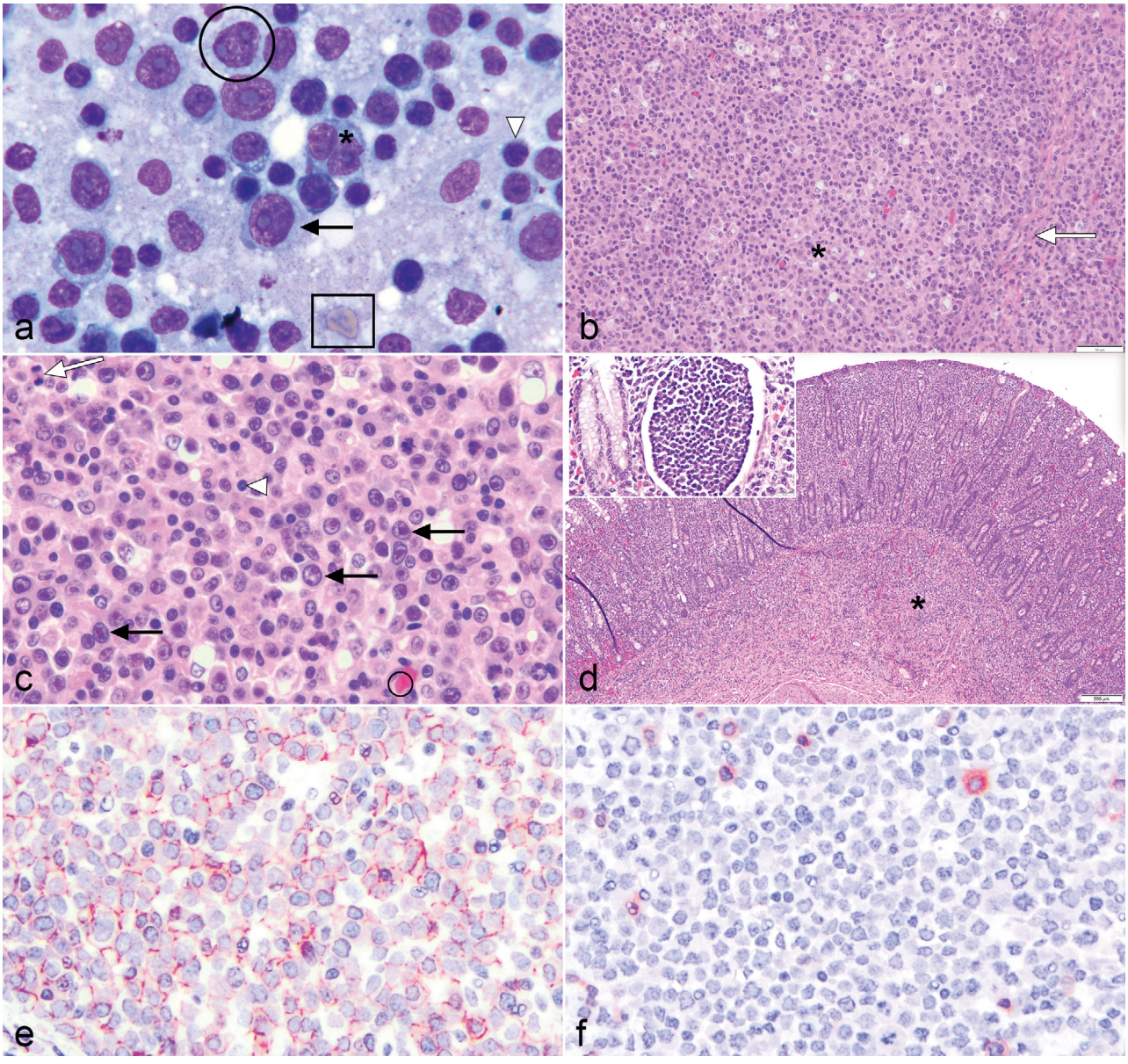

Fig. 2. (a–f) Case 1. (a) Impression of a mesenteric lymph node. Most cells have nuclei 2.5–4× the size of an erythrocyte (square), scant cytoplasm, and central nuclei with one to multiple, prominent nucleoli (arrow: single nucleolus; circle: 2 nucleoli). Binucleated cells (asterisk) are occasionally present. Small to intermediate lymphocytes also present (arrowhead). (b) Mesenteric lymph node, hematoxylin and eosin (H&E). Nodal architecture is effaced by sheets of infiltrative round cells (asterisk). Neoplastic cells have invaded through the lymph node capsule (white arrow). (c) Mesenteric lymph node, H&E. Neoplastic cells are pleomorphic round cells (black arrows) characterized by scant to moderate amphophilic cytoplasm and round to indented nucleus >2× the size of an erythrocyte (circle). There are frequent mitotic figures (white arrow). Admixed within the pleomorphic round cells are small to intermediate lymphocytes (arrowhead). (d) Colon, H&E. Mucosal lamina propria and submucosa diffusely expanded by neoplastic large lymphocytes (asterisk). Inset: Few neoplastic cells are within the colonic epithelium but often within dilated lacteals. (e) Mesenteric lymph node, immunohistochemistry (IHC) for CD20 (B cell marker). Large pleomorphic round cells have strong diffuse cytoplasmic to membranous labeling. (f) Mesenteric lymph node, IHC for CD3 (T cell marker). Numerous small to intermediate-sized lymphocytes admixed with the pleomorphic round cells have strong diffuse cytoplasmic to membranous labeling

0.237 mm^2 (1 high power field at 400×) (Meuten et al. 2016). Neoplastic cells had round nuclei with a single central nucleolus, consistent with the immunoblastic subtype. In some lymph node sections there were frequent tingible-body macrophages. The thymus in this case was also effaced by neoplastic lymphocytes, and the spleen had a nodular pattern, with periarteriolar lymphoid sheaths and lymphoid follicles expanded by large neoplastic round cells.

Case 2 had similar findings; however, not all lymph nodes were affected, and several lymph nodes had only 50% effacement by neoplastic cells. Another difference was that Case 2 had an average of 3 mitotic figures in the same field of view and neoplastic cells had folded, indented, and round nuclei with 1 or 2 central or nucleolemma-associated nucleoli. These features are more consistent with the centroblastic subtype of lymphoma. The spleen was less affected than the first case but still had a mild nodular pattern due to the neoplastic round cells. Approximately 30 to 50 percent of the bone marrow for both cases was effaced by neoplastic round cells.

There were varying degrees of epithelial invasion between organs and cases. Case 1 had the most prominent epithelial invasion in the urinary bladder while the prepuce, but not the urinary bladder, had the most severe invasion in Case 2. The ventral abdominal superficial dermis to hypodermis of Case 1 alone was effaced by neoplastic cells with invasion of hair follicles, adnexa, and epidermis and intraepithelial nests of neoplastic cells (Fig. S2b). There were also multiple ulcers with pustules, fibrinonecrotic crusts, and bacterial folliculitis. For both cases, the gastrointestinal tract had the least mucosal epithelial infiltration but did have diffuse expansion of the mucosal lamina propria as well as the gastrointestinal lymphoid tissue (GALT) by neoplastic cells (Fig. 2d). For Case 2, the oral mucosa was markedly infiltrated with neoplastic lymphocytes (Fig. S1d) causing the focus of ulceration noted on gross examination.

3.5. ICC and IHC

IHC of the postmortem lymph node impression demonstrated few small T lymphocytes with CD3 labeling, and few IBA-1 labeling macrophages. However, CD79a, a B cell marker, labeling of neoplastic cells could not be interpreted due to non-specific staining. As there were no previous reports of leukocyte antibodies used for IHC of NESs, complete evaluation of the staining was characterized. Non-specific staining was not present in the secondary-only controls. The isotype controls varied from no background staining to mild or moderate non-specific staining; however, there was no staining of neoplastic cells or small lymphocytes within affected tissues using the isotype antibodies on IHC. Of the anti-leukocyte marker antibodies applied, CD79a, a B cell marker, had the most non-specific staining (mild to moderate) of serum and smooth muscle, followed by CD20, a B cell marker, and PAX5, a B cell marker, which had mild non-specific staining. CD3, a T cell marker, and CD204, a macrophage marker, antibodies had minimal to no non-specific staining.

Within affected lymphoid organs, most of the neoplastic cells of both cases had moderate to strong cytoplasmic and membranous B cell labeling with CD20 antibodies, which comprised 50–70% of the cellular population (Fig. 2e). There was significant non-specific labeling with CD79a antibodies, and therefore it could not be interpreted (Fig. S2a). There was mild diffuse nuclear PAX5 labeling, a B cell marker, of neoplastic cells from Case 1, and moderate to strong labeling in Case 2 that comprised 75% of the infiltrative cellular population (Fig. S2b). There was strong cytoplasmic and membranous labeling of the small admixed or peripheralized lymphocytes that comprised 30–50% of the cellular population using CD3 antibody, a T cell marker, with the thymus having the greatest number (Fig. 2f). Within the medulla of the lymph nodes, but also admixed amongst neoplastic cells, were cells with CD204 labeling (Fig. S2c).

Based on the following morphologic and immunohistochemical features, i.e. diffuse lymphadenopathy, effacing infiltrative mononuclear cell population, relative sparing of the bone marrow, morphologic features of neoplastic cells, and labeling with anti-CD20 and PAX5 antibodies, diffuse large B cell lymphoma was diagnosed in both cases, with Case 1 more consistent with an immunoblastic subtype and Case 2 more consistent with a centroblastic subtype.

3.6. Viral sequencing and phylogenetic analysis and TEM

The herpesvirus sequence obtained from affected spleen and lymph node of both cases was 692 bp. The sequence was submitted to GenBank under accession number MW691977. A new virus, hereafter referred to as miroungine gammaherpesvirus 3 (MirGHV3), was detected in all affected tissues

from both cases. Bayesian model jumping found the WAG model of AA substitution was most probable, with a posterior probability of 100%. Bootstrap values from the analysis are shown on the Bayesian tree (Fig. S3). MirGHV3 clustered in the subfamily *Gammaherpesvirinae* but did not sit within any defined genus. It was found in a clade of viruses using hosts in the suborder *Caniformia*. The analysis found 100% posterior probability support for the monophyly of this clade. OtGHV3, first found in a CSL with lymphoma, is also in this clade (Venn-Watson et al. 2012). A mixture of herpesviruses including NES GHV1, were detected in the unaffected lymph node from Case 2 (Table 1). MirGHV3 was not detected in tissues from the 3 unaffected NES pups. Only NES GHV1 and PhHV6 were identified in the spleen and/or lymph nodes from these pups (Table 1). No distinct viral particles were detected by TEM in the pulmonary lymph node from Case 1.

4. DISCUSSION

The ICC and IHC antibodies used in this study to characterize leukocytes in these cases had not been previously validated for northern elephant seals. As CD20 is an early lymphocyte marker and there have been reports of canine CD3 and CD20 co-positive T cell lymphomas (Noland & Kiupel 2018), we further confirmed a B cell neoplasm in both cases by demonstrating positivity using anti-PAX5 antibodies. In this study, the efficacy and specificity of the antibody used for ICC and IHC varied and reaffirmed the importance of using isotype controls. Based on our results, CD20 and PAX5 proved to be the most reliable B cell markers while CD79a resulted in too much non-specific staining and is not recommended for use with this species. For T cells and macrophages, reliable results were obtained with CD3 and CD204, respectively.

Based on the canine World Health Organization (WHO) classification system for canine lymphoma,

Table 1. Herpesviruses detected in various tissues from lymphoma and non-lymphoma (control) northern elephant seal (NES) pups. Control NES pups were necropsied in 2019 or 2021. MirGHV3: miroungine gammaherpesvirus 3; PhGHV6: phocid gammaherpesvirus 6; NES GHV1: northern elephant seal gammaherpesvirus 1 (Gulland et al. 2018)

Seal	Cause of death	Tissue	Lesion	Herpesvirus detected
Case 1	Lymphoma	Spleen	Nodular large cell lymphoma	MirGHV3
		Axillary and mesenteric lymph nodes	Diffuse large cell lymphoma	MirGHV3
		Thymus	Diffuse large cell lymphoma	MirGHV3
		Bone marrow	Diffuse large cell lymphoma	MirGHV3
Case 2	Lymphoma	Spleen	Nodular large cell lymphoma	MirGHV3
		Tracheobronchial, inguinal and left mandibular lymph nodes	Diffuse large cell lymphoma	MirGHV3
		Right mandibular lymph node	Multifocal nodular large cell lymphoma	Mixed herpesviruses
NES Control 1	Aspiration pneumonia, malnutriton	Pulmonary lymph node	No significant microscopic findings	NES GHV1
NES Control 2	Otostrongyliasis	Spleen	Mild extramedullary hematopoiesis and hemosiderosis	None
		Mesenteric lymph node	Mild parafollicular lymphoid hyperplasia	PhGHV6
		Pulmonary lymph node	Mild follicular and parafollicular lymphoid hyperplasia with congestion	None
NES Control 3	Trauma, malnutrition	Spleen	Mild to moderate extramedullary hematopoiesis and hemosiderosis	None
		Pulmonary and mesenteric lymph nodes	Multifocal moderate parafollicular and mild follicular lymphoid hyperplasia	NES GHV1

these cases were diagnosed as diffuse large B cell lymphoma (DLBL) (Valli et al. 2011). This is the first report of this virus-associated neoplasm in monachine phocids (elephant seals, monk seals, and Antarctic phocids). Previous surveys of mortality in NES pups from a breeding colony and of pups in rehabilitation at TMMC failed to identify neoplasia of any kind (Colegrove et al. 2005, Spraker et al. 2014). As part of this study, a retrospective survey of the TMMC pathology database for a 5 yr period (January 1, 2016 to August 1, 2021) revealed no further cases among 242 NES pup necropsies. Based on the cases reported here, the prevalence of lymphoma in stranded free-ranging NES pups admitted to TMMC is approximately 0.83%. In comparison, canine lymphoma has a prevalence of 0.02–0.1% (Zandvliet 2016).

Lymphoma has previously been reported in other pinniped species including HS, CSL, NFS, and a harp seal *Pagophilus groenlandicus* (Stedham et al. 1977, Stroud & Stevens 1980, Colegrove et al. 2010, Venn-Watson et al. 2012, Malberg et al. 2017). Most of the cases were in adults, but a few were in pups or juveniles such as in these cases (Stedham et al. 1977, Stroud & Stevens 1980). Typically, lymphoma in pinnipeds can be either multicentric or restricted to a location such as lymph nodes or the intestines (Gulland et al. 2018). Of the cases in the literature with associated IHC, those restricted to the intestines were primarily comprised of intermediate neoplastic lymphocytes of T cell origin and had more prominent epitheliotropism with lesser involvement of the lamina propria or submucosa as described in our cases (Colegrove et al. 2010, Malberg et al. 2017), whereas cases of multicentric lymphoma when characterized by IHC were B cell in origin similar to our cases (Venn-Watson et al. 2012).

Lymph nodes of young pinnipeds often have scattered large blast-like lymphocytes due to a developing immune system and continuous antigenic stimulation. This should not be mistaken for lymphoma and differs from our cases in that the blast-like cells are limited to lymph node follicles and are not found in other tissues. The blast-like cells also comprise less than 20% of the total cellular population within the lymph node (Fig. S2d). A common cause of thrombocytopenia, and elevations in bilirubin and other hepatic injury markers in NES pups and yearlings, is vasculitis associated with *Otostrongylus circumlitus*, as exemplified by the bloodwork changes of Control 2 (Table S1). Neither of the lymphoma cases presented in this study had evidence of otostrongyliasis, and therefore the hepatic injury in these cases was most likely related to infiltration of the liver by neoplastic lymphocytes and the thrombocytopenia due to infiltration of the bone marrow and suspected paraneoplastic immune-mediated destruction. In comparison to otostrongyliasis, where the primary hematologic change is neutrophilia (Sheldon et al. 2019), the 2 lymphoma cases here presented with a lymphocyte differential of >50% and large lymphocytes with flower-like nuclei on blood smears.

DLBL is the most common neoplasm in dogs, with most presenting in stage IV lymphoma and having a relatively good response to treatment and median survival time, despite the aggressive behavior based on mitotic index (Aresu et al. 2015). In contrast, the current NES cases presented in Stage V, as evident by bone marrow infiltration on histology, neoplastic round cells on blood smears, persistent leukocytosis and lymphocytosis, as well as enlarged and effaced lymph nodes. Also contrary to dogs, these cases progressed swiftly and with a poorer prognosis. Furthermore, lymphoma usually presents in middle-aged to older dogs, and DLBL in humans also occurs mainly in adults (Seelig et al. 2016, Zandvliet. 2016).

Although DLBL in humans more commonly presents in adults, it can occur in pediatric patients with one of the more common forms being Burkitt's lymphoma (BL). BL is a mature B cell neoplasm characterized by the reciprocal translocation of the *c-myc* gene and typically the *IGH* gene, an immunoglobulin gene (Sandlund & Martin 2016). Human gammaherpesvirus 4 (HGHV4) in the genus *Lymphocryptovirus*, sometimes referred to as Epstein-Barr virus, is an oncogenic driver in BL, especially when co-infected with malaria, and BL is the most common type of pediatric cancer in children in sub-Saharan Africa (Casulo & Friedberg 2018). The prevalence of HGHV4-associated lymphoma is much higher following infection in marmoset or tamarin aberrant hosts than in human endemic hosts (Miller et al. 1977, Sundar et al. 1981). Another virus-induced human lymphoid neoplasm is adult T cell lymphoma/leukemia (ATL) caused by human T-cell leukemia virus, a retrovirus that is associated with 'flower-like' cells, reminiscent of the multinucleated neoplastic cells in the NES cases presented here (Panfil et al. 2016). Similarities of BL and ATL to both the present cases led to the investigation of a possible viral association with NES lymphoma.

The provenance of MirGHV3 is not known. Genetic bottlenecks often lead to significant loss of associated viral diversity (Moro et al. 2003), and it is probable that some viral diversity was lost in NESs as MirGHV3 is only the third gammaherpesvirus to have been found in the species (Fig. S3). Phocid

GHV6 was the second herpesvirus identified in elephant seals, but it was also isolated from a HS, so it is not clear which is the endemic host as both host species were housed at the same rehabilitation center (Wright et al. 2015). The other gammaherpesvirus (NES GHV1) was identified in weaned pups that developed buccal and lingual ulcers while they were patients at the same rehabilitation facility (Goldstein et al. 2006). Further surveillance for these viruses, and associated pathology, in sympatric phocid species is indicated.

In addition to their limited virome, the genetic bottleneck that affected the NES population also resulted in extremely limited major histocompatibility complex (MHC) gene diversity, which is critical for viral immunity (Weber et al. 2000). NES MHC diversity is even lower than that reported for some critically endangered terrestrial mammals (Weber et al. 2004). Inbreeding is possibly a factor in development of OtHV1-associated urogenital carcinoma in CSLs; however, more recent studies suggest that CSL urogenital carcinoma may not be as strongly associated with lack of MHC diversity as previously thought (Acevedo-Whitehouse et al. 2003, Barragán-Vargas et al. 2016, Gulland et al. 2020). MHC types also play a significant role in protection against herpesviral-associated lymphoma in chickens with Marek's disease (Smith et al. 2020). High lipid burdens of organochlorine pollutants are another significant co-factor in carcinogenesis in OtGHV1-infected CSLs (Gulland et al. 2020). While the role of legacy pollutants on lymphoma incidence or prevalence in marine mammals is unknown, preliminary studies using a HS B lymphoma cell line suggests these compounds influence the immune systems response to pathogens (Frouin et al. 2010, Kleinert et al. 2017). A hepatosplenic large cell immunoblastic lymphoma was diagnosed in a bottlenose dolphin *Tursiops truncatus* that also had high levels of similar organochloride pollutants, but the association between the 2 is speculative (Jaber et al. 2005). Further investigation of the oncogenic potential of MirGHV3 should include evaluation of tissue burdens of pollutants, in addition to genetic factors, as potential promoters.

In conclusion, a novel gammaherpesvirus was detected in tissue from NES pups with a previously undescribed lymphoma but not from unaffected controls. While the oncogenic potential for this virus remains unknown, further studies regarding the prevalence of this new gammaherpesvirus and its associated pathogenesis are necessary.

Acknowledgements. The authors thank and acknowledge Dr. C. Cray at the University of Miami's Acute Phase Protein Laboratory for the processing of serum for serum amyloid A and protein electrophoresis, A. Villareal at the University of California Davis Veterinary Medical Teaching Hospital Histology Lab for the histopathology and immunohistochemistry, and Dr. R. Cianciolo at The Ohio State University College of Veterinary Medicine for transmission electron microscopy. The authors thank the animal care, laboratory and necropsy staff and volunteers of The Marine Mammal Center who contributed to the care and diagnostic work up of this case, in particular B. Halaska, J. Isbell, and J. Poblacion. We thank the donors that support the medical and pathology research at TMMC. This work was also supported by the Aquatic Animal Health Program at the University of Florida. The Marine Mammal Center operates under NOAA permit number 18786-04.

LITERATURE CITED

Acevedo-Whitehouse K, Gulland F, Greig D, Amos W (2003) Inbreeding: disease susceptibility in California sea lions. Nature 422:35

Aresu L, Martini V, Rossi F, Vignoli M and others (2015) Canine indolent and aggressive lymphoma: clinical spectrum with histologic correlation. Vet Comp Oncol 13:348–362

Barragán-Vargas C, Montano-Frías J, Ávila Rosales G, Godínez-Reyes CR, Acevedo-Whitehouse K (2016) Transformation of the genital epithelial tract occurs early in California sea lion development. R Soc Open Sci 3: 150419

Beatty J (2014) Viral causes of feline lymphoma: retroviruses and beyond. Vet J 201:174–180

Beckmen KB, Lowenstine LJ, Newman J, Hill J, Hanni K, Gerber J (1997) Clinical and pathological characterization of northern elephant seal skin disease. J Wildl Dis 33:438–449

Buckles EL, Lowenstine LJ, Funke C, Vittore RK and others (2006) Otarine Herpesvirus-1, not papillomavirus, is associated with endemic tumours in California sea lions (*Zalophus californianus*). J Comp Pathol 135:183–189

Casulo C, Friedberg JW (2018) Burkitt lymphoma – a rare but challenging lymphoma. Best Pract Res Clin Haematol 31:279–284

Cianciolo RE, Brown CA, Mohr FC, Spangler WL and others (2013) Pathologic evaluation of canine renal biopsies: methods for identifying features that differentiate immune-mediated glomerulonephritides from other categories of glomerular diseases. J Vet Intern Med 27(Suppl 1):S10–S18

Colegrove K, Grieg D, Gulland F (2005) Causes of live strandings of northern elephant seals (*Mirounga angustirostris*) and Pacific harbor seals (*Phoca vitulina*) along the central California coast, 1992–2001. Aquat Mamm 31:1–10

Colegrove KM, Jr JFXW, Rivera R, Moore PF and others (2010) Polyomavirus infection in a free-ranging California sea lion (*Zalophus californianus*) with intestinal T-cell lymphoma. J Vet Diagn Invest 22:628–632

Davison AJ (2011) Evolution of sexually transmitted and sexually transmissible human herpesviruses. Ann NY Acad Sci 1230:E37–E49

Deming AC, Wellehan JFX, Colegrove KM, Hall A and others (2021) Unlocking the role of a genital herpesvirus, otarine herpesvirus 1, in California sea lion cervical cancer. Animals (Basel) 11:491

Fauquier D, Gulland F, Haulena M, Spraker T (2003) Biliary adenocarcinoma in a stranded northern elephant seal (*Mirounga angustirostris*). J Wildl Dis 39:723–726

Frouin H, Fortier M, Fournier M (2010) Toxic effects of various pollutants in 11B7501 lymphoma B cell line from harbour seal (*Phoca vitulina*). Toxicology 270:66–76

Goldstein T, Lowenstine LJ, Lipscomb TP, Mazet JA, Novak J, Stott JL, Gulland FM (2006) Infection with a novel gammaherpesvirus in northern elephant seals (*Mirounga angustirostris*). J Wildl Dis 42:830–835

Gulland FMD, Dierauf LA, Whitman KL (eds) (2018) CRC handbook of marine mammal medicine, 3rd edn. Taylor & Francis, Boca Raton, FL

Gulland FMD, Hall AJ, Ylitalo GM, Colegrove KM and others (2020) Persistent contaminants and herpesvirus OtHV1 are positively associated with cancer in wild California sea lions (*Zalophus californianus*). Front Mar Sci 7:602565

Jaber JR, Pérez J, Carballo M, Arbelo M and others (2005) Hepatosplenic large cell immunoblastic lymphoma in a bottlenose dolphin (*Tursiops truncatus*) with high levels of polychlorinated biphenyl congeners. J Comp Pathol 132:242–247

Katoh K, Toh H (2008) Improved accuracy of multiple ncRNA alignment by incorporating structural information into a MAFFT-based framework. BMC Bioinformatics 9:212

Kleinert C, Lacaze E, Mounier M, de Guise S, Fournier M (2017) Immunotoxic effects of single and combined pharmaceuticals exposure on a harbor seal (*Phoca vitulina*) B lymphoma cell line. Mar Pollut Bull 118:237–247

Lowry MS, Condit R, Brian Hatfield, Allen SG and others (2014) Abundance, distribution, and population growth of the northern elephant seal (*Mirounga angustirostris*) in the United States from 1991 to 2010. Aquat Mamm 40: 20–31

Malberg S, Gregersen HA, Henrich M, Herden C (2017) Epitheliotropic intestinal T-cell lymphoma in a harbor seal (*Phoca vitulina*). J Zoo Wildl Med 48:568–572

Maness HTD, Nollens HH, Jensen ED, Goldstein T and others (2011) Phylogenetic analysis of marine mammal herpesviruses. Vet Microbiol 149:23–29

Meuten DJ, Moore FM, George JW (2016) Mitotic count and the field of view area: time to standardize. Vet Pathol 53: 7–9

Miller G, Shope T, Coope D, Waters L, Pagano J, Bornkamn G, Henle W (1977) Lymphoma in cotton-top marmosets after inoculation with Epstein-Barr virus: tumor incidence, histologic spectrum antibody responses, demonstration of viral DNA, and characterization of viruses. J Exp Med 145:948–967

Miller MA, Schwartz T, Pickett BE, He S and others (2015) A RESTful API for access to phylogenetic tools via the CIPRES science gateway. Evol Bioinform Online 11: 43–48

Moro D, Lawson MA, Hobbs RP, Thompson RCA (2003) Pathogens of house mice on arid Boullanger Island and subantarctic Macquarie Island, Australia. J Wildl Dis 39: 762–771

Nicholas J (2000) Evolutionary aspects of oncogenic herpesviruses. Mol Pathol 53:222–237

Noland EL, Kiupel M (2018) Coexpression of CD3 and CD20 in canine enteropathy-associated T-cell lymphoma. Vet Pathol 55:241–244

Panfil AR, Martinez MP, Ratner L, Green PL (2016) Human T-cell leukemia virus-associated malignancy. Curr Opin Virol 20:40–46

Rajčáni J, Asványi-Molnár N, Szathmary S (2010) Herpesvirus-associated lymphomas: investigations in humans and animal models. Acta Microbiol Immunol Hung 57: 349–376

Ronquist F, Teslenko M, van der Mark P, Ayres DL and others (2012) MrBayes 3.2: efficient Bayesian phylogenetic inference and model choice across a large model space. Syst Biol 61:539–542

Rosenwirth B, Kondova I, Niphuis H, Greenwood EJD and others (2011) Herpesvirus saimiri infection of rhesus macaques: a model for acute rhadinovirus-induced t-cell transformation and oncogenesis. J Med Virol 83: 1938–1950

Sandlund JT, Martin MG (2016) Non-Hodgkin lymphoma across the pediatric and adolescent and young adult age spectrum. Hematology (Am Soc Hematol Educ Program) 2016:589–597

Seelig DM, Avery AC, Ehrhart EJ, Linden MA (2016) The comparative diagnostic features of canine and human lymphoma. Vet Sci 3:11

Sheldon JD, Hernandez JA, Johnson SP, Field C, Kaye S, Stacy NI (2019) Diagnostic performance of clinicopathological analytes in *Otostrongylus circumlitis*-infected rehabilitating juvenile northern elephant seals (*Mirounga angustirostris*). Front Vet Sci 6:134

Smith J, Lipkin E, Soller M, Fulton JE, Burt DW (2020) Mapping QTL associated with resistance to avian oncogenic Marek's disease virus (MDV) reveals major candidate genes and variants. Genes (Basel) 11:1019

Spraker TR, Lyons ET, Kuzmina TA, Tift MS, Raverty S, Jaggi N, Crocker DE (2014) Causes of death in preweaned northern elephant seal pups (*Mirounga angustirostris*, Gill, 1866), Año Nuevo State Reserve, California, 2012. J Vet Diagn Invest 26:320–326

Spraker TR, Kuzmina TA, Lyons ET, DeLong RL, Simeone C, Veeramachaneni DNR (2019) Multifocal necrotizing myopathy in northern elephant seal (*Mirounga angustirostris*) pups, San Miguel Island, California. Vet Pathol 56:143–151

Stedham MA, Casey HW, Keyes MC (1977) Lymphosarcoma in an infant northern fur seal (*Callorhinus ursinus*). J Wildl Dis 13:176–179

Stroud RK, Stevens DR (1980) Lymphosarcoma in a harbor seal (*Phoca vitulina richardii*). J Wildl Dis 16:267–270

Sundar SK, Levine PH, Ablashi DV, Leiseca SA and others (1981) Epstein-Barr virus-induced malignant lymphoma in a white-lipped marmoset. Int J Cancer 27:107–111

Trupkiewicz JG, Gulland FM, Lowenstine LJ (1997) Congenital defects in northern elephant seals stranded along the central California coast. J Wildl Dis 33:220–225

Valli VE, Myint M, Barthel A, Bienzle D and others (2011) Classification of canine malignant lymphomas according to the World Health Organization criteria. Vet Pathol 48: 198–211

VanDevanter DR, Warrener P, Bennett L, Schultz ER, Coulter S, Garber RL, Rose TM (1996) Detection and analysis of diverse herpesviral species by consensus primer PCR. J Clin Microbiol 34:1666–1671

Venn-Watson S, Benham C, Gulland FM, Smith CR and others (2012) Clinical relevance of novel Otarine herpesvirus-3 in California sea lions (*Zalophus californianus*): lymphoma, esophageal ulcers, and strandings. Vet Res 43:85

Weber DS, Stewart BS, Garza JC, Lehman N (2000) An empirical genetic assessment of the severity of the northern elephant seal population bottleneck. Curr Biol 10:1287–1290

Weber DS, Stewart BS, Schienman J, Lehman N (2004) Major histocompatibility complex variation at three class II loci in the northern elephant seal. Mol Ecol 13: 711–718

Wright EP, Waugh LF, Goldstein T, Freeman KS and others (2015) Evaluation of viruses and their association with ocular lesions in pinnipeds in rehabilitation. Vet Ophthalmol 18(Suppl 1):148–159

Zandvliet M (2016) Canine lymphoma: a review. Vet Q 36: 76–104

Editorial responsibility: Michael Moore, Woods Hole, Massachusetts, USA
Reviewed by: C. Suárez-Santana, A. Deming and 1 anonymous referee

Submitted: October 25, 2021
Accepted: March 10, 2022
Proofs received from author(s): May 3, 2022